Hybridization of Al and O states in alpha- and gamma-alumina

1993 J. Phys.: Condens. Matter 5 8629

(http://iopscience.iop.org/0953-8984/5/45/016)

J. Phys.: Condens. Matter 5 (1993) 8629–8642. Printed in the UK

Hybridization of Al and O states in α- and γ-alumina

M Kefi†, P Jonnard†, F Vergand†, C Bonnelle† and E Gillet‡

† Laboratoire de Chimie Physique Matière et Rayonnement, Université Pierre et Marie Curie, 11 rue Pierre et Marie Curie, 75231 Paris Cédex 05, France

‡ Laboratoire de Microscopie et Diffractions Electroniques, 13397 Marseille Cédex 20, France

Received 26 July 1993

Abstract. The partial Al and O valence spectral densities of α- and γ-alumina in bulk and in the superficial zone of the samples are investigated using x-ray emission spectroscopy induced by electrons. These valence states are mixed over the whole width of the band. We show that changes in the atomic environment affect the hybridization of states in a narrow energy range. For the γ-phase and superficial zones of the two phases, increased hybridization is observed. This is correlated with an increase in the covalent character of Al–O bonds at the surface and the γ-phase. Defect states are observed both in the gap between O 2s and O 2p states and in the optical gap; for the α-phase, a structure is seen at about 1 eV above the top of the valence band which we interpret as due to an oxygen-vacancy state.

1. Introduction

Aluminium oxide is widely used in various applications because it is chemically inert and insulating and has a small expansion coefficient. For example, it is used as protection against corrosion, as a substrate in catalysis and as an insulator for thermocouples or in metal–ceramic multimaterials.

The technological importance of Al_2O_3 has stimulated many investigations of its bulk and surface electronic properties. Valence densities of states (DOSs) have been investigated by x-ray photoelectron spectroscopy (XPS) and ultraviolet photoelectron spectroscopy (UPS). No differences have been observed between α-alumina, γ-alumina and amorphous alumina using XPS [1, 2], which probes the total valence DOS weighted by the photoabsorption cross section in a thin layer at the surface of the sample. In fact, because of photoionization cross sections, the x-ray photoelectron spectrum of Al_2O_3 is dominated by the O 2s DOS which is not very sensitive to small changes in the local atomic arrangement. Recently ultraviolet photoelectron spectra have been reported for α- and γ-alumina [3] which show changes attributed to the difference between the Al coordination values of these phases.

Partial Al and O DOSs of Al_2O_3 have already been reported using electron-induced x-ray emission spectroscopy (EXES). Experiments were performed with powdered [4, 5] or single-crystal α samples [6]. The mixing of partial DOSs, the role of the crystal structure and the depth probed were not discussed.

For a compound such as Al_2O_3, the bond has a partially covalent character. This can be evidenced from the analysis of partial Al and O valence DOSs. It has been predicted that the covalence varies at the surface. Moreover one expects the DOS to change with the crystal structure. Such changes must remain weak and can be seen only from partial DOSs.

In this paper, we present an EXES study of partial Al and O DOSs for various alumina samples which are to be used as substrates in ceramic–metal systems. Mixing of Al and O

0953-8984/93/458629+14$07.50

states is discussed in relation to the theoretical DOSs. Attention is given to changes observed for the γ- and α-phases and for the bulk and a superficial zone of the samples of about a hundred ångströms.

Radiative recombination from states located in the band gap can also be observed by EXES. Structures of this type are seen in the Al 3p spectral density and an interpretation is proposed.

The samples and the experimental procedure are described in section 2. The results are presented and discussed in sections 3 and 4.

2. Samples and method of analysis

2.1. The samples

The atomic arrangement of α-alumina has rhombohedral symmetry (space group, D_{3d}^6), and two Al_2O_3 formula units are present in the unit cell [7]. The lattice is usually described as a slightly deformed hexagonal cell of oxygen atoms, three times as large as the rhombohedral cell and whose c axis is along the main diagonal of the latter. All the aluminium atoms are located at octahedral sites; thus they are surrounded by six oxygen atoms; for three of them the nearest-neighbour distance is 1.97 Å and for the three others it is 1.86 Å.

For γ-alumina the structure is that of an inverse spinel (space group, O_h^7) where oxygen atoms form a FCC lattice [7]. There are eight Al_2O_3 formula units per cell. The parameter a is equal to 7.9 Å. Aluminium atoms are located in both tetrahedral and octahedral sites.

Thus it is important to note that α- and γ-alumina have different coordination values of the Al atoms, namely, 6 in α-alumina and both 4 and 6 in γ-alumina.

We studied samples of α- and γ-alumina of various origins. One kind of α-alumina sample consisted of small single-crystal platelets with the faces parallel to the (0001) plane. We analysed them in three forms.

(i) As received, just slightly cleaned: these small plates are supplied by CRYSTAL-TEC (Centre d'Etudes Nucléaires Grenoble) with surfaces mechanically polished so that their structure is polycrystalline to a depth of about 1 μm. These α-alumina samples will be referred to as polished samples in the following.

(ii) Cleaned by a moderate heat treatment (589 °C) and ion bombardment (Ar^+; 1 keV; 10 μA in an UHV chamber (base pressure, 2.6×10^{-10} mbar) in oxygen at 1.3×10^{-6} mbar). Such samples do not give a LEED pattern [8]. We consider that they are still polycrystalline to a depth of 1 μm.

(iii) Treated by a heat treatment after the above cleaning. The samples are annealed at 1000 °C for 1 or 2 h until a (1 × 1) LEED pattern is obtained [8]. The surface is thus single crystal.

The other kind of α-alumina that we used was small polished plates with the faces parallel to the ($\bar{1}012$) planes, supplied by CRYSTAL-TEC. The polishing makes the samples polycrystalline to a depth of about 1 μm.

We studied two types of polycrystalline γ-alumina. One of these was prepared at the Office National d'Etudes et Recherches Aéronautiques (ONERA) by RF sputtering in Ar at 10^{-2} mbar. Deposits of γ-alumina 4 μm thick were obtained on a Ni-based alloy at 780 °C. The other type was a powdered γ-alumina purchased from Johnson–Matthey.

2.2. Methods of analysis

Radiative recombinations are observed subsequently to the creation of a hole in an inner subshell. In EXES, the core holes are created by incident electrons. This method is depth selective and must be used in the study of deep metal–Al_2O_3 interfaces [9]. Moreover, it makes the analysis of the excited-state recombination possible. These are the reasons why we have chosen this ionization mode.

Only electrons which have an energy higher than the ionization threshold E_s of the subshell are effective in the emission process. The thickness in which the electrons have an energy higher than E_s is referred to as the emissive thickness. For each sample, the Al 3p–1s emission is observed from two different emissive thicknesses. This is possible by using two values for the incident electron energy E_0. We have chosen 2 and 4 keV. The Al 1s ionization threshold $E_{Al\ 1s}$ is determined by adding the energies of Al Kα (2p–1s) emission and of the Al 2p ionization, obtained by XPS for that sample. For γ-Al_2O_3, we obtain 1561.4 eV. The average energy of the incident electrons was about 400 or 2400 eV higher than the threshold energy.

Exact determination of the emissive thickness is difficult. Using the empirical law generally accepted to describe the slowing down of electrons in matter [10], we have estimated the lengths that the electrons go through with an energy between E_0 and $E_{Al\ 1s}$; they are 200 Å and 1300 Å, respectively. The emissive thicknesses are estimated in the incidence direction and are clearly smaller than this path length. Moreover the number of effective electrons, i.e. electrons having an energy higher than the threshold energy, decreases rapidly with increasing depth. The ionization cross section decreases also strongly at threshold. Finally, alumina is a large-gap insulator and a charge effect is present on the surface; the incident electrons (3 mA cm^{-2}) are repelled and their path length decreases. Consequently, we attribute the spectra obtained at 2 keV to the emission from a superficial zone of the sample of about 100 Å and the spectra at 4 keV to the emission from the bulk. The superficial zone is clearly thinner than the superficial contamination.

Our study is performed by means of a Johann-type spectrometer with a bent-crystal (500 mm radius) monochromator described elsewhere [11]. The Al 3p–1s emission lies in the photon energy range from 1530 to 1560 eV and is analysed with a $(10\bar{1}0)$ quartz crystal. The O 2p–1s emission lies in the 515–530 eV region and is analysed with TlAP (001). For each element, a change in the physicochemical characteristics of the sample gives an energy shift of approximately the same value for all the levels and the x-ray emissions are observed at the same photon energy.

Spectra densities are plotted on a binding energy scale which is referred to the top of the valence band E_v. For Al 3p–1s and O 2p–1s, E_v is determined by the usual method, i.e. by extrapolating the linear part of the emission towards the higher photon energy (the lower binding energy) (cf figure 1). Such a procedure introduces an uncertainty estimated at 0.2 eV. The emission Al 3s–2p is plotted with the same binding energy scale by adjusting the top of the valence band, determined, independently in [6]. The ordinates are proportional to the number of emitted photons. The background is subtracted and the curves are normalized with respect to their maximum amplitude.

XPS measurements were carried out in an UHV chamber equipped with an Al Kα x-ray source (1486.6 eV) and with an hemispherical analyser (VSW HAC 100). The resolution limit of the spectrometer is in the range of 0.6 eV for a pass energy of 25 eV.

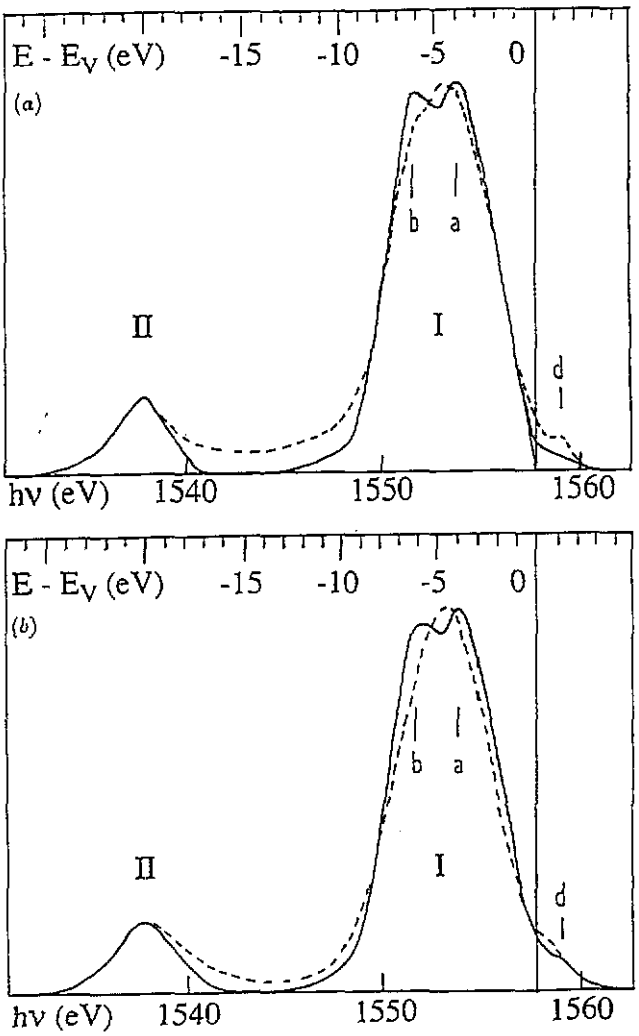

Figure 1. Al 3p–1s electron-induced x-ray emission spectra in α-Al_2O_3 (Al 3p spectral density versus binding energy with respect to the top of the valence band). (*a*) Polished samples; ——, bulk; – – –, superficial zone. (*b*) Treated samples: ——, bulk; – – –, superficial zone.

3. Results

3.1. α-Al_2O_3

The Al 3p–1s emission of clean α-$Al_2O_3(0001)$ is plotted in figure 1, and the bulk and the superficial zone are compared. The spectral density spreads over about 25 eV. The main peak is composed of two structures Ia and Ib, located at −4 eV and −6 eV respectively, below E_V. These two structures are of equal importance for the bulk whilst, for the superficial zone, peak Ia is more intense than Ib. In both spectra, peak II is observed at −20 eV from E_V. In the bulk, no intensity is observed between peaks I and II. This energy range is often labelled the 'ionic gap'.

The same Al 3p–1s spectral density is observed for polished α-$Al_2O_3(0001)$ and $(\bar{1}012)$.

For treated α-Al_2O_3(0001) (cf figure 1), the spectral density of the bulk is the same as that observed before treatment. In contrast, the emission from the superficial zone is different from that of other samples; as seen in the figure, peak Ib is less well resolved and peak I is narrower; its width is about 5.6 eV. Indeed the treated sample is single crystal in the superficial zone and not in the bulk.

Faint structures are observed close to and above E_v. They are at the same energy for all samples but their intensity is larger for the treated sample than for the others.

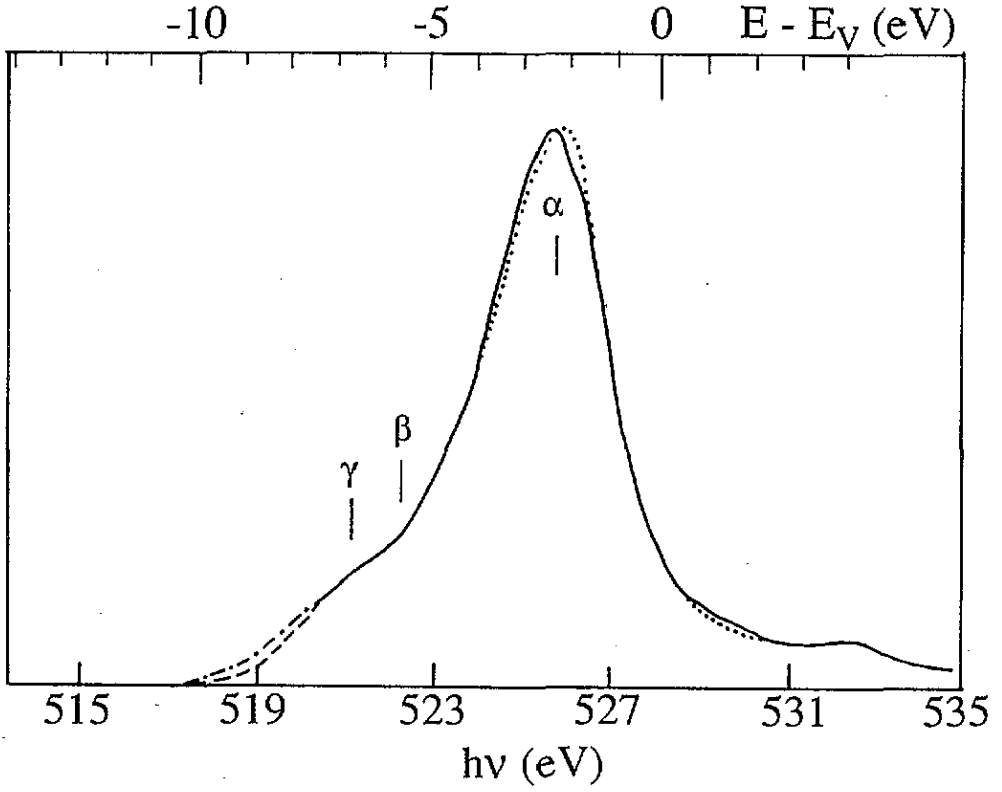

Figure 2. O 2p–1s electron-induced x-ray emission spectra (O 2p spectral density versus photon energy): ——, γ-Al_2O_3; ·····, α-Al_2O_3.

The O 2p–1s emission of the polished sample is plotted in figure 2. The spectrum is not corrected for the anomalous reflectivity of the monochromator which is relatively weak and located towards the higher-photon-energy side, at 532.5 eV. The O 2p–1s spectral density spreads over the same binding energy range as peak I of Al 3p, i.e. about 11.5 eV. A non-structured main peak 3 eV wide, labelled α, is observed at -2.9 eV below E_v; this peak decreases abruptly towards low binding energies and is strongly asymmetric towards high energies. A feature, labelled γ, is observed at -7.5 eV. We label the position between the main peak α and the shoulder γ as β.

3.2. γ-Al_2O_3

The Al 3p–1s emission for the ONERA sample is plotted in figure 3 for the bulk and the superficial zone. The general characteristics, such as the spreading of the spectral density,

the position of peaks I and II and the absence of states between peaks I and II for the bulk, are the same as for $\alpha-Al_2O_3$. In contrast, the peaks Ia and Ib are not well resolved and peak Ib is clearly less intense than peak Ia. For the superficial zone, the decrease in the intensity of peak Ib is even clearer, the main part of peak I is narrower than for the bulk and the spectral density is always different from zero. No structure is observed close to and above E_v.

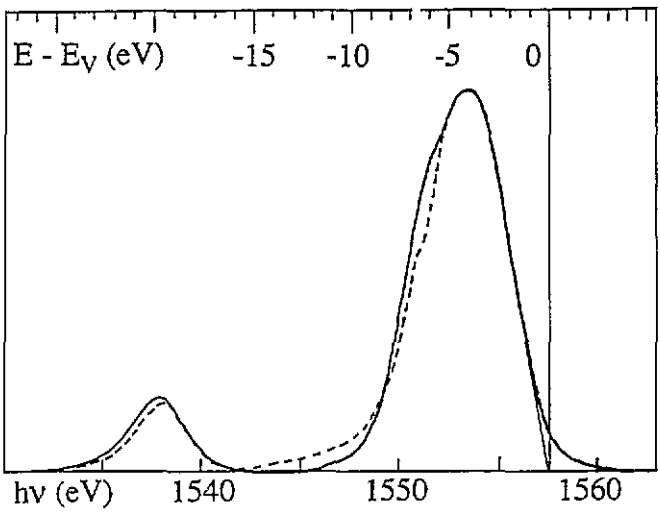

Figure 3. Al 3p–1s electron-induced x-ray emission spectra in γ-Al_2O_3 (Al 3p spectral density versus binding energy with respect to the top of the valence band.): ——, bulk; – – –, superficial zone.

The Al 3p–1s emission of the Johnson–Matthey sample has the same characteristics as the ONERA sample except for the presence of a self-absorption effect which is specific to powdered samples. Indeed, because the surface is rough, the emitted photons can be reabsorbed in the direction of observation and a decrease in the photon number is observed at the energy of the 1s absorption threshold. We have determined the variation in the product of the thickness and the photoabsorption cross section at the threshold. From this curve, we have located the threshold energy at 1564.2 eV. It is at +6.8 eV above E_v. This value corresponds to the width of the band gap for this sample. It is clearly smaller than the value of 8.5 eV determined by photoconductivity for single-crystal α-Al_2O_3.

The Al emission of bulk γ-Al_2O_3 is shown in figure 4 together with the bulk cleaned α-Al_2O_3(0001) sample. The various peaks are at the same energies but clear differences are seen in the detailed shape of peak I.

The O 2p–1s emission for the ONERA sample is plotted in figure 2. Its shape is very similar to that observed for α-Al_2O_3(0001) with the main peak slightly shifted towards higher binding energies. A very faint feature is observed at +1.5 eV above the top of the valence band.

4. Discussion

4.1. Comparison between the spectral DOSs of bulk α-Al_2O_3

In figure 5, we compare the Al 3p and O 2p spectral densities of the bulk α-Al_2O_3(0001) with

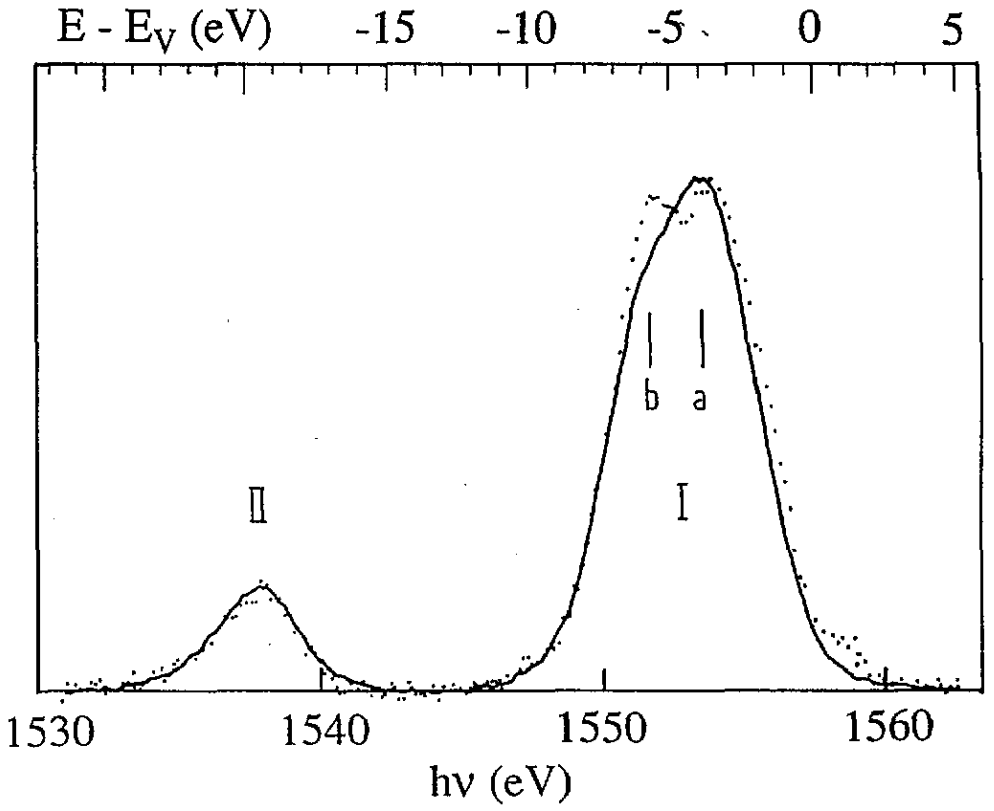

Figure 4. Al 3p–1s electron-induced x-ray emission spectra (Al 3p spectral density versus photon energy for bulk): ——, γ-Al_2O_3; · · · · · ·, α-Al_2O_3.

the Al 3s spectral density obtained by EXES for the bulk [6] and with the x-ray photoelectron spectrum. The latter describes the total valence DOS weighted by the photoionization cross section and the analysed thickness is some tens of ångströms. The electron distribution spreads over the same energy range.

We first compare Al 3p and 3s spectral densities. Peak Ia of Al 3p coincides with the main peak of Al 3s; the Al s and p DOSs are thus strongly hybridized in this region of the valence band. In contrast, peak Ib of Al 3p corresponds approximately to a minimum B in the Al 3s spectral density. Thus, in this region, the Al DOSs have a predominantly 3p character. No peak is present in the 3p spectral density at the position of the secondary peak C of the 3s spectral density. Peak II of Al 3p coincides with the faint peak D of the Al 3s DOS. These results confirm that hybridization of Al 3s and 3p states is present over the total width of the valence band to a more or less large extent. Indeed the states are predominantly p between 5 and 6.5 eV and predominantly s between 6.5 and 7.5 eV.

In the comparison between Al and O spectral densities, it must be emphasized, first of all, that the O 2p spectral density extends over the same energy range as the main peak of the Al s–p densities. This is an important result because it shows that the shapes of the O 2p and Al 3sp DOSs are interdependent. Towards low binding energies, the edges of the Al and O spectral densities are at the same position but their shapes are different. The edge of the O 2p DOS is clearly more abrupt than that of the Al DOS and the main O 2p peak is narrow. Thus the main part of the O 2p DOS lies just at the top of the valence band. It

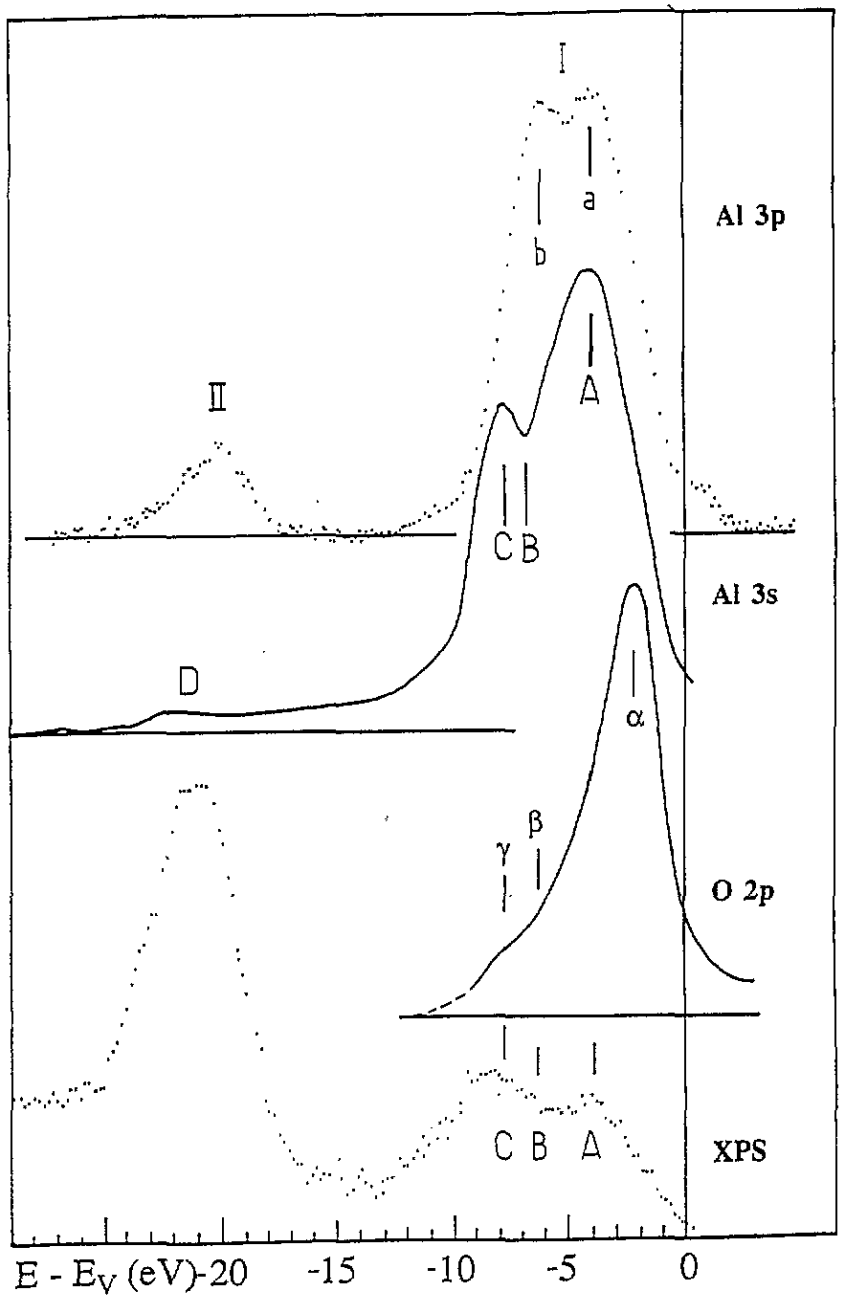

Figure 5. Partial spectral densities for α-Al_2O_3 as obtained by EXES compared with total spectral density as obtained by XPS. Al 3p, O 2p and XPS were from the present work and Al 3s from [6].

should be noted that the difference between the shapes observed for the Al and O edges could be partially due to the lifetimes of inner holes. In fact the Al 1s level (0.4 eV) is wider than the O 1s level (0.1 eV) and one expects the Al 3p edge to be broadened with

respect to the O 2p edge.

The position β of O 2p is at the same energy as peak Ib of Al 3p. This result confirms that the Al peak Ib corresponds to predominant Al 3p states. The feature γ of O 2p coincides with the peak C of Al 3s, the corresponding states being hybridized O 2p–Al 3s states. This hybridization of Al and O states is responsible for the spreading of O 2p DOS towards higher binding energies.

Peaks D and II of Al 3s and Al 3p DOSs, respectively, coincide with the high-binding-energy XPS peak. This XPS peak corresponds essentially to the O 2s spectral density. Consequently, peaks D and II are due to the hybridization between Al 3s–3p and O 2s states.

The total valence DOS obtained by XPS has the same energy range as the partial Al 3s and 3p DOSs observed by EXES but the relative insensities of parts I and II of the valence band are very different. This is due to transition probabilities. The photoionization cross section increases with increasing electron localization close to the nucleus and it is larger for O 2s than for O 2p, Al 3s and Al 3p. Then the main XPS peak corresponds to predominant O 2s states which have a behaviour close to that of an inner shell. The lower-energy part of the total valence DOS (0–10 eV) is strongly structured. By comparing the total DOS with the partial DOS, we have identified the states which contribute to the various XPS features; because the photoionization cross section of Al 3s states is larger than that of Al 3p and also O 2p states, the two main features of the XPS spectral density correspond to two peaks of Al 3s DOS and the intensity of the O 2p peak is relatively weak. As for the Al 3p DOS, it contributes little to the spectral density.

4.2. Comparison between the experimental and theoretical DOSs of α-Al_2O_3(0001)

The valence DOSs of α-alumina have been calculated by different methods [12–17]. From these results, the valence band extends over two clearly spaced energy regions: the lower valance band (LVB) and upper valence band (UVB).

Only local (Al or O) and partial (s or p) DOSs can be compared directly with our experimental data. From one of the first calculations [14], using the extended Hückel method, it has been shown that the O 2s and 2p and Al 3s and 3p DOSs spread over both the LVB and the UVB. In this calculation, the band structure has been optimized by introducing for the fundamental gap the value deduced from photoconductivity measurements. Consequently, the widths of the various bands are in agreement with those of the spectral densities, making the calculated DOSs directly comparable with the experimental data.

From recent calculations using self-consistent methods, only the local DOSs are determined. As an example, the total and Al and O DOSs of α-Al_2O_3 have been determined from the orthogonalized linear combination of atomic orbitals OLCAO method in the local-density approximation [15]. The general shapes of the local DOSs are analogous to those previously obtained; in particular a large peak in the O 2p DOS is found near the top of the valence band and the Al 3s and 3p DOSs are small. On the other hand, the widths of the LVB and UVB as well as those of the band gaps are underestimated and clearly reduced with respect to the experimental values. Such a result is generally found for the wide-gap insulators and not for the covalent semiconductors. This can be due to difficulties in taking into account the partial ionic character of the binding which is present in these insulators.

We show in figure 6 the Al and O s and p DOSs for α-Al_2O_3(0001) from [14]. The curves are adjusted with respect to E_v and can be compared directly with the spectral densities plotted in figure 5. The shape of the partial O 2p DOS is in good agreement with our experimental curve. The Al 3s DOS spread over the lower parts of both the LVB and

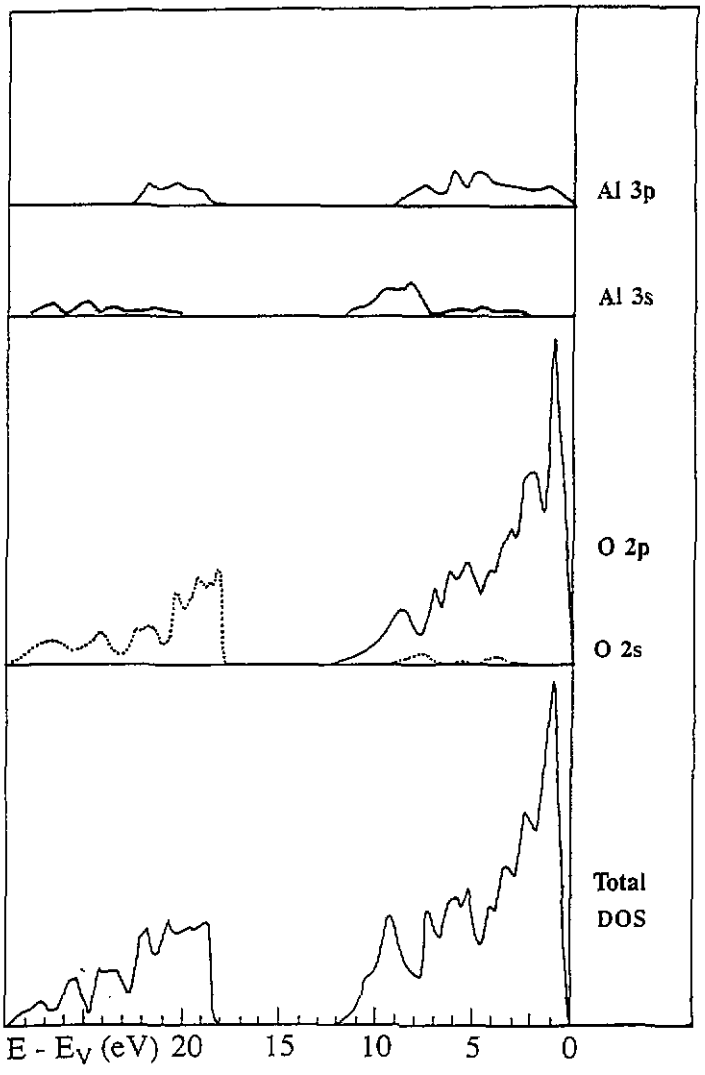

Figure 6. Calculated DOSs for α-Al_2O_3 [13].

the UVB, and the Al 3p DOS over their higher parts, as seen experimentally. These results show that the many-body effects are negligible in the valence spectral densities of alumina. However, the detailed shape of the calculated Al 3s and 3p DOSs is not in good agreement with the experimental curves; in particular, no maximum is present in the calculated Al 3s DOS near the top of the valence band.

It must be emphasized that, although the Al DOSs are small, they contribute strongly to the shape of the total DOS through their hybridization with the O 2p states.

4.3. Changes with the crystal structure

The O 2p and Al 3p of bulk cleaned α-Al_2O_3(0001) and γ-Al_2O_3 are shown in figures 2 and 4.

First, we shall compare the Al 3p spectral DOSs. The most significant difference concerns the intensity of peak Ib. In α-Al_2O_3, the Al atoms are present only in octahedral sites while, in γ-Al_2O_3, they are present simultaneously in octahedral and tetrahedral sites. In a tetrahedral site, one expects the presence of sp^3 hybrid orbitals; a covalent character is associated with this type of orbital. Then the covalent character of the binding must be larger in γ- than in α-Al_2O_3. An increase in the hybridization is associated with an increase in the covalent character; thus a decrease in the features corresponding to pure or slightly hybridized states occurs. As shown above, peak Ib of Al 3p is at the same energy as the minimum B and the minimum β of Al 3s and O 2p spectral densities. Consequently this peak corresponds to slightly hybridized states and we interpret its decrease as an increase in the covalent character of the binding in γ-Al_2O_3.

A small change in the low-energy edge is observed for the Al 3p and O 2p spectral DOSs. The edge is less abrupt, making the maximum slightly shifted towards high binding energies for γ-Al_2O_3 with respect to α-Al_2O_3. The changes are the same for both Al 3p and O 2p DOSs. This result confirms that the Al and O p states interact in this range of DOSs.

No change is seen for peak II for Al 3p. From [6], the same result is verified for the Al 3s spectral DOS. From the total DOS seen by UPS [3], for γ-Al_2O_3 the spectral density increases between peaks A and C and the minimum B is not observed. These changes correspond to an increase in the Al 3s DOS in this range and are in agreement with a decreased intensity of slightly hybridized Al 3p states.

In summary, the main spectral change associated with the crystal structure involves peak Ib of the Al 3p spectral DOS. The hybridization is weak in the energy range of this peak because the other spectral DOSs have a minimum at its vicinity. This energy range is thus very sensitive to a variation in the mixing of states. Consequently, a decreasing intensity of the peak Ib can be considered as characteristic of increasing covalent character of the bond in alumina.

It should be noted that a small change in the relative intensities of peaks Ia and Ib as a function of the polarization of the emitted radiation has been seen for single-crystal α-Al_2O_3 [18]. The spectra were recorded with the trigonal c axis of the single-crystal α-Al_2O_3 either parallel or perpendicular to the reflection plane of the spectrometer crystal. From these spectra, the emitted intensities $I_\parallel$ and $I_\perp$ with the polarization vector parallel or perpendicular to the trigonal c axis of the sample were deduced. The intensities $I_\parallel$ and $I_\perp$ correspond predominantly to transitions from non-bonding and bonding valence states, respectively. Peak Ib was slightly more pronounced for $I_\parallel$ than for $I_\perp$. Thus peak Ib corresponds predominantly to transitions from non-bonding states, i.e. only slightly or unhybridized states, in agreement with our conclusion. In our experiments, the sample is fixed. The Bragg angle is 69.74°, giving a polarization ratio of about 0.6–0.7. Moreover the (0001) surface of the sample is inclined by 10° with respect to the focalization plane which slightly increases the depolarization effect. Then the decrease in peak Ib observed for the surface of α-Al_2O_3 cannot be related to a polarization effect.

4.4. Comparison between the DOSs of the bulk and of the superficial zone

4.4.1. Cleaned α-Al_2O_3. The Al 3p spectral DOS of the superficial zone is presented in figure 1 and compared with that of the bulk. Two types of changes are observed: the shape of the main peak is different and supplementary states are present between −10 and −16 eV.

Concerning the main peak, for the superficial zone, the intensity of peak Ib decreases. As discussed in the previous section, this change is characteristic of an increase in covalency.

From the Al 3p spectral DOS we show that the Al–O binding is more covalent in the superficial zone than in the bulk. This result is in agreement with a theoretical study which predicts an increase in the covalent character of the binding because tetrahedral arrangements are present at the surface [14].

Calculation of the valence DOS for Al in a tetrahedral environment has shown that cation–cation wrong bonds introduce states in the ionic gap [19]. Consequently, we interpret the supplementary states present in this energy range, i.e. between peaks I and II of the Al 3p spectral DOSs as being due to this type of defect.

4.4.2. Treated α-Al_2O_3. Changes of the same type are observed for the superficial zone of the treated sample. Concerning the main peak, the changes are more marked after treatment; peak Ib is not well resolved and the maximum of peak I becomes narrower towards high binding energies. This suggests that the proportion of Al atoms having a fourfold coordination increases during the treatment. This result is in agreement with the study made by LEED, AES and XPS on the surface of these same samples [20]. Between peaks I and II, the spectral density and also the defect state density are smaller than in the cleaned sample.

4.4.3. γ-Al_2O_3. The same changes are observed but they are more marked than for α-Al_2O_3 (see figure 3). Peak Ib has a strongly decreased intensity and is slightly shifted towards high binding energies; it coincides with the minimum B. This indicates that the tetrahedral sites are rather numerous at the surface of the γ-phase. The increase in the spectral density between peaks I and II reveals that defect states are present at the surface of the γ sample.

For all the samples, the spectral density observed in the superficial zone between peaks I and II varies from 2 to 4% of the main peak. As discussed above, we interpret the spectral density observed in this range as due to the presence of cation–cation wrong bonds in the total depth of the superficial zone.

4.5. Low-energy structures

A structure is observed in the Al 3p spectral density of α-Al_2O_3 towards low binding energies, i.e. high photon energies, at about +1 eV above the top of the valence band. Its intensity varies with the sample and is a few per cent of peak I. This structure is not a satellite emission from doubly excited or ionized states. In fact, for Al metal, no satellite is seen at this energy and no supplementary satellite can exist at this energy for a large-gap insulator such as alumina.

Features due to the radiative recombination from states located in the band gap can be observed in this energy range. These states are either excitonic states or donor or acceptor defect states. In the x-ray range, donor states can be observed only through a recombination process. Acceptor states can be populated simultaneously to the creation of the inner hole; they can be observed through excitation spectroscopies such as x-ray or ultraviolet photoabsorption and electron energy loss spectroscopy.

Excitonic states are expected to be close to the bottom of the conduction band so that the structure observed at +1 eV above E_v cannot be an excitonic transition. We suggest that this feature is due to the radiative recombination from a defect state.

A low-energy structure has been observed in the electron energy loss spectrum of the same samples at 5.3 eV and is interpreted as an excitation transition from the valence band to a defect state [20]. The energy difference between the maximum of the Al 3p peak Ia and structure d is approximately 5 eV. Thus a correspondence exists between the structure d seen in the Al emission spectrum and that observed in the excitation spectrum.

The energies of defect states associated with oxygen vacancies have been calculated [14]. These states are located +0.8, +6.2 and +7.5 eV above E_v. Consequently, the Al 3p structure d can be interpreted as due to a defect state associated with oxygen vacancies. Treatment increases the number of oxygen vacancies slightly. In the spectrum of superficial zones, another very weak feature is observed about +0.2 eV above E_v. This could be due to charged oxygen vacancies. On the other hand, in the γ-phase, structure d is not observed but a structure is present in the O 2p spectrum. This suggests that other defects are present in this sample. Experiments are in progress to study these low-energy structures.

5. Conclusion

The EXES analysis of Al and O partial spectral DOSs of alumina reveals that the mixing of valence states has not got the same strength over the whole width of the band. The peak at −6 eV below E_v in the Al 3p partial DOS is characteristic of slightly hybridized states. Its intensity varies strongly with the atomic environment and this peak can be used to characterize the covalency of the bond. From our observations, the covalency is more important for γ-Al_2O_3 than for α-Al_2O_3. It increases at the surface with respect to the bulk. This increase of the covalency takes place over a depth of about 50 Å.

On the other hand, the mixing between O 2p and Al 3s and 3p states is responsible for the shape of the O 2p DOS. The Al 3s and 3p states spread over about 10–12 eV in the metal and various compounds. The O 2p valence distribution is broader in alumina than, for example, in alkaline-earth oxides for which the width of the DOS of the metallic element is known to be only a few electron volts.

We have observed a defect state in the band gap of all the α-Al_2O_3 samples. We have identified it as a state associated with an oxygen vacancy. EXES experiments are in progress to study such defects.

Acknowledgment

The authors thank Dr Magali Cléry who prepared the ONERA samples.

References

[1] Balzarotti A and Bianconi A 1976 *Phys. Status Solidi* b **76** 689
[2] Kowalczyk S P, McFeely F R, Ley L, Gritsyna V T and Shirley D A 1977 *Solid State Commun.* **23** 161
[3] Frederick B G, Apai G and Rhodin T N 1991 *Surf. Sci.* **244** 67
[4] Sénémaud C 1966 *J. Physique Coll.* **27** C2 55
[5] Urch D S 1970 *J. Phys. C: Solid State Phys.* **3** 1275
[6] Brytov A and Romashchenko Yu N 1978 *Sov. Phys.–Solid State* **20** 384
[7] *Landolt-Börnstein New Series* 1955 *Kristalle (Atom und Molekularphysik 4)* (Berlin: Springer)
[8] Gillet E 1991 *Science of Ceramic Interfaces* ed J Nowotny (Amsterdam: Elsevier) p 439
[9] Kefi M, Jonnard P, Vergand F, Amamou A and Bonnelle C 1993 *Interface Sci.* at press
[10] Fitting H J 1974 *Phys. Status Solidi* a **26** 525
[11] Bonnelle C *et al* 1993 to be published
[12] Reilly M H 1970 *J. Phys. Chem. Solids* **31** 1041
[13] Tossel J A 1975 *J. Am. Chem. Soc.* **97** 4840; 1975 *J. Phys. Chem. Solids* **36** 1273
[14] Ciraci S and Batra P 1983 *Phys. Rev.* B **28** 982
[15] Xu Yong-Nian and Ching W Y 1991 *Phys. Rev.* B **43** 4461
[16] Guo J, Ellis D E and Lam D J 1992 *Phys. Rev.* B **45** 3204

[17] Guo J, Ellis D E and Lam D J 1992 *Phys. Rev.* B **45** 13647
[18] Dräger G and Leiro J A 1990 *Phys. Rev.* B **41** 12919
[19] O'Reilly E P and Robertson J 1986 *Phys. Rev.* B **34** 8684
[20] Gillet E and Ealet B 1992 *Surf. Sci.* **273** 427